Journal of Materials Science and Engineering with Advanced Technology
Volume 2, Number 1, 2010, Pages 11-25

A MODEL ALUMINA BASED INVESTMENT CASTING CERAMIC CORE BODY SYSTEM

YEXIA QIN and WEI PAN

Industrial Technology Research Institute
South China University of Technology
Guangzhou, 510641
P. R. China
e-mail: qinyexia@gmail.com

State Key Laboratory of New Ceramics and Fine Processing
Department of Materials Science and Engineering
Tsinghua University
Beijing, 100084
P. R. China

Abstract

A family of alumina ceramic core composites sintered at 1300°C, 1400°C, and 1500°C for 5h were in situ synthesized and characterized to understand its complex behavior. The sintered product exhibits a microstructure consisting of in situ synthesized $Al_{2(1-x)}Mg_xTi_{(1+x)}O_5$ phase throughout the predominant α-Al_2O_3 matrix. The ceramic cores of theoretical 20wt% in situ synthesized $MgTi_2O_5$ contents show excellent phase stability in temperature regimes, where Al_2TiO_5 generally undergo severe phase decomposition. Thermal expansion coefficients as low as 2.4×10^{-6}/K (24°C to 1000°C) were observed. The low thermal expansion is attributed to a combination of the microcracking, the porosities, and the phase stability. The ceramic cores of theoretical 20wt% in situ synthesized $MgTi_2O_5$ contents sintered at 1500°C for 5h have almost no creep

Keywords and phrases: ceramic core composites, property, investment casting, alumina-based, in situ synthesized.

Received April 4, 2010

deformation in the present research. With proper processing, the composites represent a low thermal expansion, high-temperature stability, and almost no creep deformation makes them potential candidates for commercial applications for investment casting.

1. Introduction

In the casting of hollow articles, of intricate shapes, such as blades and vanes used in gas turbine engines for aircraft applications using both single crystal and polycrystalline directional solidification investment casting techniques, ceramic cores are used [11, 12]. These ceramics must satisfy the following requirements [14, 15]:

(i) Chemical compatibility with the molten metal, low creep, and resistance to thermal shock.

(ii) High porosity (> 20%), can be leached from the cooling cavity of the hollow castings with water, NaOH, or dilute hydrochloric acid.

(iii) Having high strength and low shrinkage characteristics, in order to retain the highly precise shape and size of the cast part.

Most commercial cores used for the production of hollow metal castings contain fused silica. Fused silica is used because, it maintains sufficient strength at casting temperature and may be removed after casting from within the cast article by leaching with molten caustic soda or aqueous hydrofluoric acid [3].

To achieve higher efficiency in a gas turbine engine, it is well known that the operating temperature of the engine must be increased. However, the increase in gas turbine engine operating temperatures is limited by the availability of high temperature materials capable of withstanding these increased operating temperatures.

In the power plants for missiles, turbine drives and aircraft engines, use is made of blades, vanes, and other structural parts that are required to withstand extremely high temperature, under extremely high temperature, under extremely corrosive conditions. A new generation of

high-melting-point superalloys, which allow higher operating temperatures in the range from about 1480˚C to about 1600˚C and, hence, higher efficiencies to be achieved in gas turbine engines, has been developed. While many of these superalloys are reactive with conventional fused silica cores, they present problems in that conventional silica-based ceramic cores can not withstand the higher temperatures at which these materials are cast [5]. It is recognized that, there is a demand for a ceramic core that has excellent thermal shock resistance, strength, thermal expansion, excellent leachability, and remains dimensionally and chemically stable at casting temperatures in excess of 1480˚C [4, 7]. However, relatively inexpensive raw materials are expected to form such a ceramic core so that, it is economical to use cores formed of the material in large scale production. To achieve the foregoing objects, it is necessary to develop a new kind of ceramic core materials with higher properties. Recent developments in making ceramic cores have concentrated on composition modification and the related processing technology [10]. The technology of making ceramic cores as well as casting metals, however, is either retained as proprietary information or protected by patents.

To achieve optimal properties of the cast components for the aerospace industry, adequate materials properties, and dense and homogeneous packing of powders as well as evenly distributed additives are required. To achieve the foregoing objectives, it is necessary to develop a new kind of ceramic core material with higher properties. Because of its low thermal expansion coefficient $(0.2 \times 10^{-6}$ to 1×10^{-6} $K^{-1})$, and excellent thermal shock resistance $(\sim 500\ W \cdot m^{-1})$, sintered aluminum titanate (Al_2TiO_5, tialite) is a ceramic with different potential applications. An important limitation to the application of this material is represented by its tendency to decompose into the parent oxides below 1280˚C, according to the reaction [2]

$$Al_2TiO_5 \rightarrow \alpha - Al_2O_3 + TiO_2 - \text{rutile}. \quad (1)$$

In order to make full use of the excellent properties and control the decomposition of the aluminum titanate, it is necessary to study the ceramic cores of theoretical in situ synthesized solid solution of $Mg_xAl_{2(1-x)}Ti_{(1+x)}O_5$ contents, and the proper sintering process. In this paper, a series of alumina based ceramic core composites were prepared adopting in situ synthesized method. The microstructure and the properties of alumina-based ceramic core composites are discussed.

2. Experimental Procedures

Corundum powder, TiO_2- rutile, and magnesia powders were mixed in the desired molar ratio. The alumina powder is used in forming the ceramic core material includes both coarse and fine particles. The coarse particle remains substantially un-reacted during sintering of the core. A carbon-bearing fugitive filler material was used for a degree of porosity sufficient to provide for crushability of the core. Raw materials were mixed with a slow-speed stirrer at 50r.p.m. for 30 minutes. Mixtures were then dried. The powders, obtained in this way, were used as starting materials to synthesize the solid solutions of $Al_{2(1-x)}Mg_xTi_{(1+x)}O_5$. Three different powders were obtained. The compositions of samples are listed in Table 1.

Table 1. Composition and character of raw materials of ceramic cores

Composition	TiO_2- rutile (wt%)	MgO (wt%)	Al_2O_3 (wt%)
T1	9	0	91
T2	17	2	81
T3	25	4	71

The admixtures were pressed into pellets by dry-pressing, and then were reaction-sintered at 1300, 1400, and 1500˚C for 5 hours in air. The phase identification of the specimens was carried out by X-ray powder diffraction analysis (XRD; D/max－RB) with CuKα radiation. The microstructures of the cross-sections after sintering were observed by

using scanning electron microscopy (SEM; JSM-6460LV) operating at 20KV. A coating of a thin conducting layer of Au-Pd or carbon was found necessary. Sintered densities (ρ) of all specimens were measured with the Archimedes principle by using deionized water as the immersion medium according to ASTM C373 [1].

The thermal expansion of the sintered samples between room temperature and 1000˚C during heating was measured by using the dilatometer at a constant heating rate of 6˚C/min up to 1000˚C. The test apparatus was modified electronically from a 1977 Netzsch test unit for refractoriness under load and creep in compression.

The creep deformation of the sintered alumina core was evaluated by cantilever test. Rectangular bars with dimensions of 3mm × 4mm × 45mm were prepared for testing creep property. Each bar was cantilevered in a furnace and heated at 200˚C/h to 1500˚C for 3h hold at temperature.

Phase decomposition was evaluated on sintered bars by isothermally heating samples at 1100˚C for 10h. The degree of decomposition of the annealed specimens was determined from the specific intensity, $\frac{I_{Al_2TiO_5}}{I_{Al_2TiO_5} + I_{TiO_2}} \times 100\%$, which was obtained by measuring the XRD peak area of d_{023} of Al_2TiO_5 and d_{101} of TiO_2 [9, 16].

The sintered cores were leached by using a standard hot aqueous caustic solution at 80˚C. The microstructures and EDS results of each core composition were recorded before and after testing.

3. Results and Discussion

3.1. Microstructure and phase composition

Representative XRD patterns of the samples sintered at 1500˚C for 5h used in the current study are shown in Figure 1. It is found that the reaction products were predominantly α- Al_2O_3 and the solid solution $Al_{2(1-x)}Mg_xTi_{(1+x)}O_5$. The other oxide, such as rutile TiO_2, magnesia,

and its compounds were not detected by XRD. It is believed that the rutile TiO_2 particles contained in the core react and chemically combine with both the finer Al_2O_3 and the MgO particles. The $MgTi_2O_5$ phase forms very rapidly at the beginning of the reaction, even at 1000°C, according to the reaction [8]:

$$MgO + 2TiO_2 \rightarrow MgTi_2O_5 \quad (2)$$

with complete conversion of the MgO present in the mixture. The MgO particles are also added to limit the grain growth of the Al_2O_3 materials and, in particular, the coarse Al_2O_3 particles by preventing growth of the coarse particles at the expense of adjacent fine particles.

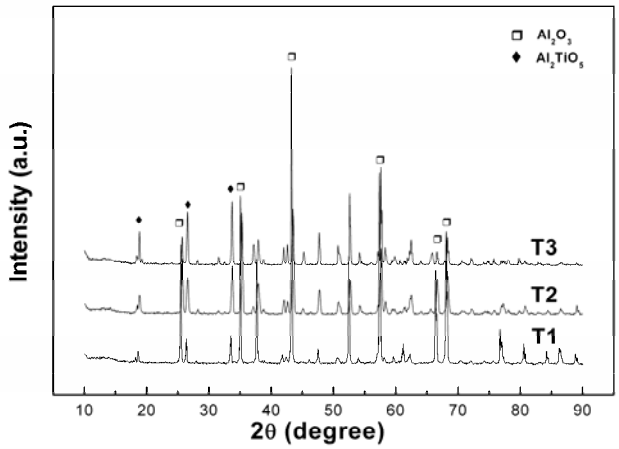

Figure 1. XRD patterns of samples sintered at 1500°C for 5h.

The formation of Al_2TiO_5 in solid solution with $MgTi_2O_5$ occurs by conversion of the fine Al_2O_3 and TiO_2 particles dispersed in the $MgTi_2O_5$–rich solid solution matrix already formed according to [13]:

$$Al_2O_3 + TiO_2 \rightarrow Al_2TiO_5. \quad (3)$$

However, reaction 3 is quite slow in comparison with reaction 2 and has to occur by solid state diffusion through the $MgTi_2O_5$ matrix. Four different mechanisms are possible: counter-diffusion of Al^{3+} and Ti^{4+} parallel diffusion of Al^{3+} and O^{2-}, parallel diffusion of Ti^{4+} and O^{2-}, and parallel diffusion of the faster moving cation and electrons coupled with oxygen transport in the gas phase. A schematic illustration of the microstructural development of reaction-sintered $MgTi_2O_5$, the Al_2O_3 and TiO_2 phase assemblage, and the formation of $Al_{2(1-x)}Mg_xTi_{(1+x)}O_5$ is given in Figure 2. Due to the superficial of the formation of $MgTi_2O_5$, the fine Al_2O_3 and TiO_2 particles penetrate into the $MgTi_2O_5$ particle surface, leading to the formation of Al_2TiO_5 in solid solution with $MgTi_2O_5$, and a degree of shrinkage. We believe that sintering takes place by the solid TiO_2 particles and MgO particles (Figure 2a). Then, Al^{3+} ions may diffuse further within the TiO_2 particles until the stochiometrical mullite composition is achieved (Figure 2b). The particles of TiO_2 and fine Al_2O_3 form contact points allowing species transport and giving rise to the formation of neck areas, which is typical of a solid-state sintering [6]. Formation of mullite at the neck areas leads to the build-up of a stiff skeleton, which cannot shrink further. This may explain the formation of a porous structure.

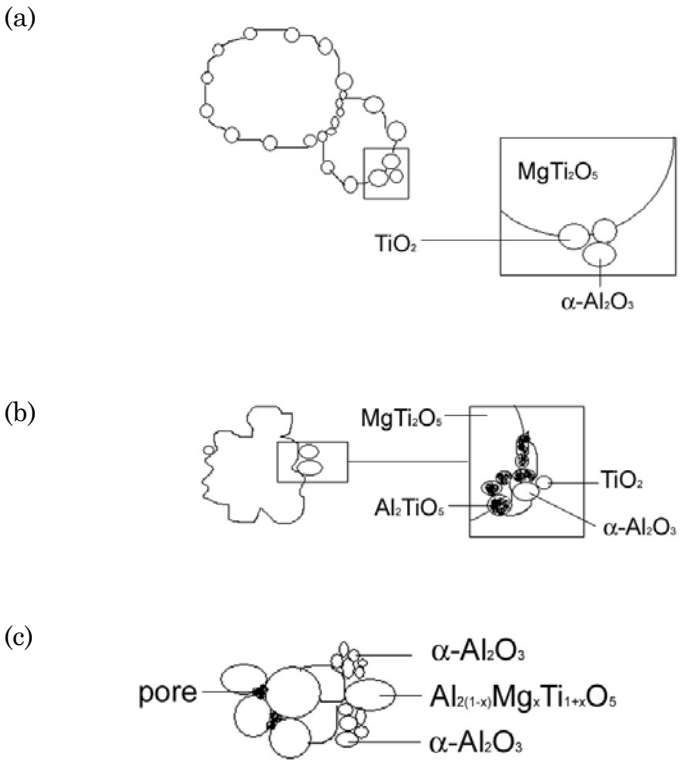

Figure 2. Schematic illustration of reaction sintering process demonstrating sintering mechanism: the formation of (a) $MgTi_2O_5$, (b) Al_2TiO_5, and (c) $Al_{2(1-x)}Mg_xTi_{(1+x)}O_5$.

The typical microstructures of the samples, containing in situ synthesized $MgTi_2O_5$ and sintered at 1500°C for 5h are compared in Figure 3. Microstructural observations revealed the grain of the product is inhomogeneous and the grain size is about several micrometers. Porosities indicating differential sintering, as shown in Figure 3, can easily be found from the sintered ceramic core samples. As can be seen in Figure 3, the microstructure of the core is characterized by the presence of substantially unreacted Al_2O_3 particles having a polycrystalline composition consisting essentially of in situ synthesized $Al_{2(1-x)}Mg_x$ $Ti_{(1+x)}O_5$ on the surface of the Al_2O_3 particles. It is believed that the

polycrystalline composition of $Al_{2(1-x)}Mg_xTi_{(1+x)}O_5$ is formed primarily on the surface of the substantially unreacted Al_2O_3 particles because, the fine Al_2O_3 particles react at a faster rate during thermal processing than do the coarse Al_2O_3 particles. Thus, the coarse Al_2O_3 particles remain substantially unreacted during sintering. As a result, coarse Al_2O_3 particles sintering will take place for the samples as the formation of the solid solution is almost already completed in the powders.

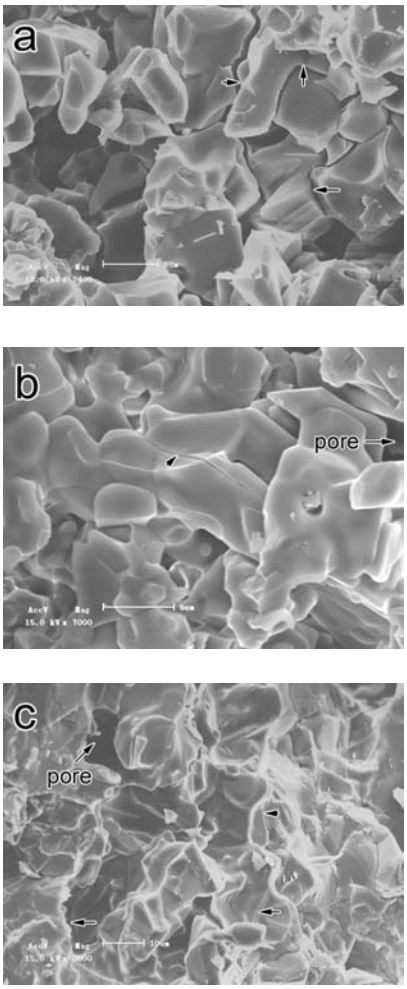

Figure 3. Representative microstructures of (a) T1, (b) T2, and (c) T3 sintered at 1500˚C for 5h showing intergranular microcracks (arrow).

Microcracks, as indicated by the arrow in Figure 3, were observed as expected due to the presence of the highly anisotropic Al_2TiO_5 phase. The presence of some multigrain microcracks, often transgranular rather than intergranular, is clearing evident in Figure 3. This is an important difference in comparison to ceramic containing no magnesium oxide. Solid solutions of sample T1 prepared from the same raw materials show predominantly intergranular microcracks. The reasons for this different behavior are currently not clear. The thermal expansion anisotropy of the pseudobrookite structure, the porosities and the phase stability are responsible for the low thermal expansion of the material.

During sintering, the carbon-bearing fugitive filler material is burned clearly out of the core. As a result, an interconnected network of porosity is created in the sintering core (Figure 3). The porosity in the core aids both the crushability and leachability of the core after casting and inhibits recrystallization of the alloy. Thus, the core should include an amount of porosity sufficient to allow the core to be leached from the casting by using standard hot aqueous caustic solutions in a reasonable period of time.

The relative density (ρ_{rel}) and shrinkage versus sintering temperature of the different samples sintered at 1300, 1400, and 1500˚C for 5h are reported in Table 2. The theoretical densities (ρ_{TD}) were calculated for each composition by assuming a fully dense ceramic free of residual pores was taken as a reference. As shown, the relative density of all the sintering temperatures for samples displayed in Table 2 increases with an increase $MgTi_2O_5$ contents in alumina-based ceramic cores. All specimens almost show the same trend at 1300, 1400, and 1500˚C. For the T1 sample, after 1300˚C sintering for 5h, no significant progress of the densification is observed. The extent of length shrinkage is 0.98% for T1 sample, 1.09% for T2 sample, and 1.52% for T3 sample. The length shrinkage in the T1 sample amounts to 4.66% sintered at 1500˚C for 5h. The T1 sample has a lower density and shrinkage than the T2 and T3 samples for temperature <1500˚C.

Table 2. Properties of samples sintered at different temperature for different time

	Shrinkage (wt%)			Relative density (wt%)		
Sample No.	1300˚C	1400˚C	1500˚C	1300˚C	1400˚C	1500˚C
T1	0.98	2.65	4.66	62.32	65.29	69.74
T2	1.09	2.55	4.60	62.35	66.87	71.12
T3	1.52	3.38	5.56	63.95	68.10	71.54

3.2. Phase stability

Table 3 shows the samples demonstrated phase decomposition ratios at 1100˚C for 10h in air. The addition of MgO, i.e., the in situ synthesized $MgTi_2O_5$ in quantities of 20wt% gave the Al_2TiO_5 almost complete phase stability in isothermal testing. No evidence of α- Al_2O_3 or TiO_2 was detected by X-ray diffraction after such testing. The replacement of Mg^{2+} for Al^{3+} in the Al_2TiO_5 structure was expected because of solid solubility between Al_2TiO_5 and $MgTi_2O_5$. Therefore, one explanation for the differences in Al_2TiO_5 content in these compositions could be that the presence of Mg^{2+} in small amounts was able to create a stable structure, which could not accommodate the smaller Al^{3+}. And, the presence of Mg^{2+} in small amounts is quite effective in reducing the thermal decomposition rate. The stability of this structure is illustrated by the complete lack of phase decomposition after exposure at 1100˚C for 10h. Such exposures generally result in extensive decomposition of Al_2TiO_5 into Al_2O_3 and TiO_2.

Table 3. Decomposition ratios of samples T1, T2, and T3

Sample No.	Decomposition ratio (%)
T1	22.8
T2	2.5
T3	0

3.3. Creep deformation and thermal expansion

The thermal expansion behaviors of specimens sintered for 5h at 1500˚C are reported in Table 4. The average value of the thermal expansion coefficient between R.T. and 900˚C is 5.1×10^{-6}/K for T1 sample, 3.2×10^{-6}/K for T2 sample, and 2.4×10^{-6}/K for T3 sample. The smaller thermal expansion coefficient of the T3 sample in comparison with the T1 and T2 samples can be related to the presence of $MgTi_2O_5$ phase and to a higher phase stability. The increase of $MgTi_2O_5$ phase content can lead to an increase in the crack volume and the phase stability and, as a consequence, to a decrease of the thermal expansion coefficient.

The creep deformation was measured after testing and shown in Table 4. It can be seen from Table 4 that, the creep deformation decreases with increase of sintering temperature. The creep deformation of ceramic core of 20wt% $MgTi_2O_5$ content sintering at 1500˚C is very little. The proper quantities of in situ synthesized $MgTi_2O_5$ wt% promote sintering and phase stability and result in a smaller creep deformation.

Table 4. Thermal expansion coefficient of samples sintered at 1500℃ and creep deformation sintered at different temperature for 5h

Sample	Thermal expansion coefficient (10^{-6}/K)		Creep deformation (mm)	
No.	20~900˚C	900~1200˚C	1400˚C	1500˚C
T1	5.1	6.0	1	0.1
T2	3.2	3.5	0.8	-
T3	2.4	2.7	0.6	-

3.4. Leaching result

The alumina cores were leached by using a caustic solution at 80˚C and the typical microstructures of T1 and T2 (sintered at 1500˚C for 5h), obtained by SEM/EDS, are shown in Figure 4. The microstructures of samples are very different from each other before and after leaching.

Figure 4a and 4b display the leached microstructure and EDS of the sample T1 sintered at 1500˚C for 5h, the microstructure of the core is characterized by the presence of substantially unreacted α-Al_2O_3 particles, and a little $NaAlO_2$ and $Al_{2(1-x)}Mg_xTi_{(1+x)}O_5$. The leaching results Figure 4c and 4d show that, the microstructure of the core is characterized by the presence of substantially $Al_{2(1-x)}Mg_xTi_{(1+x)}O_5$, a little $NaAlO_2$ and α-Al_2O_3 particles.

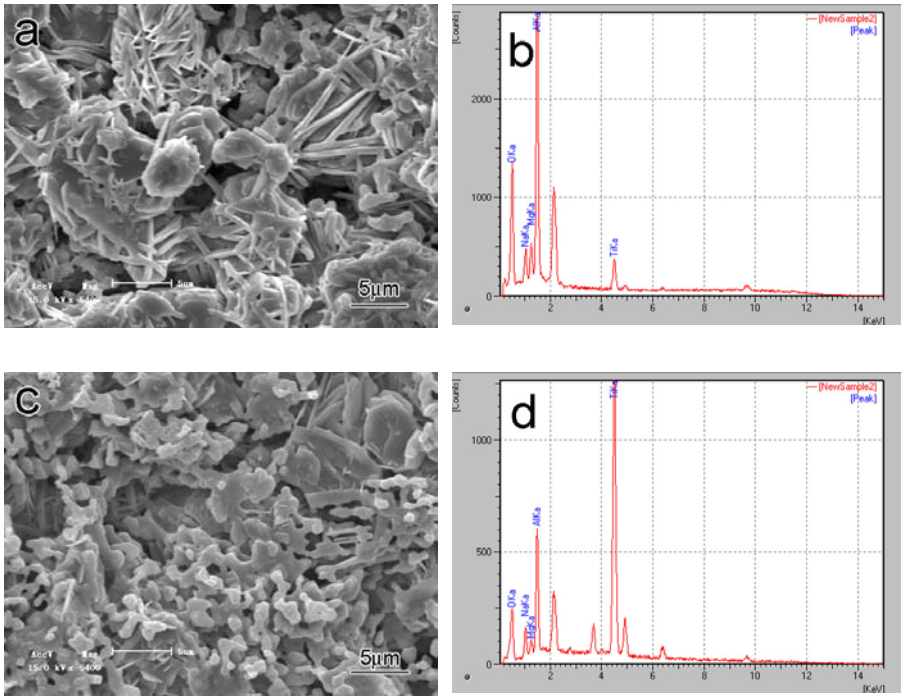

Figure 4. SEM images of (a) T1 and (c) T2, and EDS for the (b) T1 and (d) T2 after leaching test.

4. Conclusion

(1) The alumina ceramic core composites were obtained through in situ reaction of fine alumina, TiO_2, and MgO during sintering.

(2) The finest Al_2O_3 particles react at a faster rate during thermal processing than do the coarse Al_2O_3 particles to facilitate the formation of the polycrystalline composition consisting essentially of in situ synthesized $Al_{2(1-x)}Mg_xTi_{(1+x)}O_5$ on the surface of the Al_2O_3 particles.

(3) The ceramic cores of 20wt% in situ synthesized $MgTi_2O_5$ content sintered at 1500°C for 5h with a lowest thermal coefficient ($\approx 2.4\times10^{-6}/K$) has almost no creep deformation in the present research.

References

[1] ASTM Standard, Standard Test Method for Water Absorption, Bulk Density, Apparent Porosity, and Apparent Specific Gravity for Fired Whiteware Products, Annu. Book. ASTM Standard, Vol. 15.02, 112-13, ASTM International, West Conshohocken, PA, 1990.

[2] V. Buscagolia and P. Nanni, Decomposition of Al_2TiO_5 and $Al_{2(1-x)}Mg_xTi_{(1+x)}O_5$ ceramics, J. Am. Ceram. Soc. 81(10) (1998), 2645-2653.

[3] G. R. Frank, K. A. Canfield and T. R. Wright, Alumina-Based Core Containing Yttria, U. S. Pat. No. 4837187, (1989).

[4] C. D. Greskovich and R. C. Davies, Alumina-Based Ceramic for Core Materials, U. S. Pat. No. 4156614, (1977).

[5] C. Huseby, M. P. Borom and C. Greskovich, High temperature characterization of silica-base cores for superalloys, Am. Ceram. Soc. Bull. 58(4) (1979), 448-452.

[6] S. M. Johnson and J. A. Pask, Role of impurities on formation of mullite from kaolinite and Al_2O_3-SiO_2 mixtures, Am. Ceram. Soc. Bull. 61 (1982), 838-842.

[7] K. Kato and Y. Nozaki, Ceramic core for precision castings manufactured by injection molding, Imono 63 (1991), 155-160.

[8] Y. C. Ko and J. T. Lay, Thermal expansion characteristics of alumina-magnesia and alumina-spinel castables in the temperature range 800-1650°C, J. Am. Ceram. Soc. 83(11) (2000), 2872-2874.

[9] I. Masayuki, S. Tsugio, E. Tadashi and S. Masahiko, Synthesis and thermal stability of aluminum titanate solid solutions, J. Am. Ceram. Soc. 70(2) (1987), 69-71.

[10] Y. X. Qin, A. B. Du, R. Zhang and W. Pan, Aluminum-based ceramic core nano-composites for investment casting, Rare Metal Materials and Engineering 36(1) (2007), 774-776.

[11] R. R. Robb, C. Yaker and L. B. Urd, Ceramic Cores for Manufacturing Hollow Metal Castings, U. S. Pat. No. 4190450, (1980).

[12] J. Ronald and S. Rodney, Ceramic Core and Method of Making, U. S. Pat. No. 6578623, (2003).

[13] B. Saruhan, W. Albers, H. Schneider and W. A. Kaysser, Reaction and sintering mechanisms of mullite in the systems cristobalite/α-Al_2O_3 and amorphous, J. Euro. Ceram. Soc. 16 (1996), 1075-1081.

[14] C. Shaw, Silica-based ceramic cores, Foundry Trade J. 78(31) (1946), 1534.

[15] K. Steven, Ceramic Core for Investment Casting and Method for Preparation of the Same, U. S. Pat. No. 5468285, (1995).

[16] G. Tiloca, Thermal stabilization of aluminium titanate and properties of aluminium titanate solid solution, Mater. Sci. 26 (1991), 2809-2814.

■